

An Open Ocean Trial of Controlled Upwelling Using Wave Pump Technology

ANGELICQUE WHITE

College of Oceanic and Atmospheric Sciences, Oregon State University, Corvallis, Oregon

KARIN BJÖRKMAN AND ERIC GRABOWSKI

School of Ocean and Earth Science and Technology, University of Hawaii at Manoa, Honolulu, Hawaii

RICARDO LETELIER

College of Oceanic and Atmospheric Sciences, Oregon State University, Corvallis, Oregon

STEVE POULOS, BLAKE WATKINS, AND DAVID KARL

School of Ocean and Earth Science and Technology, University of Hawaii at Manoa, Honolulu, Hawaii

(Manuscript received 25 November 2008, in final form 23 September 2009)

ABSTRACT

In 1976, John D. Isaacs proposed to use wave energy to invert the density structure of the ocean and pump deep, nutrient-rich water into the sunlit surface layers. The basic principle is simple: a length of tubing attached to a surface buoy at the top, and a one-way valve at the bottom can be extended below the euphotic zone to act as a conduit for deep water. The vertical motion of the ocean forces the attached valve to open on the downslope of a wave and close on the upslope, thus generating upward movement of deep water to the surface ocean. Although Isaacs's wave-powered pump has taken many forms, from energy production to aquaculture to the more recent suggestion that artificial upwelling could be used to stimulate primary productivity and carbon sequestration, the simple engineering concept remains the same. In June 2008, the authors tested a commercially available wave pump (Atmocean) north of Oahu, Hawaii, to assess the logistics of at-sea deployment and the durability of the equipment under open ocean conditions. This test was done as part of an experiment designed to evaluate a recently published hypothesis that upwelling of water containing excess phosphate (P) relative to nitrogen (N) compared to the canonical "Redfield" molar ratio of 16N:1P would generate a two-phased phytoplankton bloom. The end result of this field experiment was rapid delivery (<2 h for a 300-m transit) of deep water to the surface ocean followed by catastrophic failure of pump materials under the dynamic stresses of the oceanic environment. Wave-driven upwelling of cold water was documented for a period of ~17 h, with a volumetric upwelling rate of ~45 m³ h⁻¹ and an estimated total input of 765 m³ of nutrient-enriched deep water. The authors discuss the deployment of a 300-m wave pump, the strategy to sample a biogeochemical response, the engineering challenges faced, and the implications of these results for future experiments aimed at stimulating the growth of phytoplankton.

1. Introduction

The vertical displacement of waves can be employed to transfer deep, nutrient-rich water to the surface of the ocean using a rather simple pump design originally conceived by Isaacs et al. (1976). A modern version of this concept is depicted in Fig. 1. It consists of a vertical

pipe attached to a free-floating surface buoy. A valve that opens and closes at opposite phases of a wave cycle is installed at the bottom end of the pipe. As the buoy moves down the surface of a wave, the valve opens and water is entrained in the pipe. On the following upslope, inertial forces move entrained water upward and deep water is eventually transferred to the surface. Upwelling velocities and total volumetric inputs generated by these pumps are a function of the amplitude and frequency of waves as well as the dimensions and efficiency of the individual pump (Liu and Jin 1995; Vershinsky et al. 1987).

Corresponding author address: Angelicque White, College of Oceanic and Atmospheric Sciences, 104 COAS Administration Building, Oregon State University, Corvallis, OR 97331-5503.
E-mail: awhite@coas.oregonstate.edu

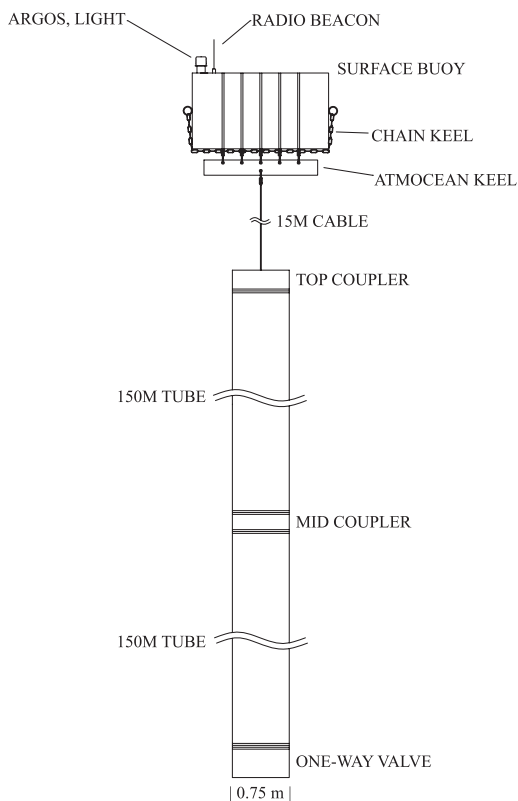


FIG. 1. The components and configuration of the wave pumps deployed north of Oahu, Hawaii, in June 2008. Dimensions of each pump are shown; however, the diagram is not to scale, because the lengths of the tubes are considerably greater than their widths.

Although wave pumps have only been successfully deployed as a small-scale means to generate power (Isaacs et al. 1976), a variety of other applications have recently been proposed, including increasing primary productivity and fish production (Kenyon 2007; Kirke 2003), fueling aquaculture (Liu and Jin 1995), and mitigating climate change via enhancement of oceanic carbon sequestration (Lovelock and Rapley 2007). Each of these proposals requires pumps that would remain operational in the open ocean long enough to generate and sustain phytoplankton blooms. The minimum operational time scale needed will depend on the pump efficiency, the number of pumps deployed, and the physical and chemical characteristics of the target region. Given our present understanding of phytoplankton bloom dynamics, this time scale is likely to be on the order of weeks to months. In addition, these proposals assume a predictable biological response of the upper ocean to deep water additions. For this reason, small-scale risk assessments of the feasibility of artificial upwelling coupled to careful measurements of the response of ocean biota are required to confirm the underlying principle

that forms the basis for each of these plans: that a wave pump could function long enough to stimulate and sustain enhanced primary productivity. The Ocean Productivity Perturbation Experiment (OPPEX) was designed and implemented to evaluate the feasibility of inducing a phytoplankton bloom in the oligotrophic open ocean.

OPPEX hypothesis and objectives

The North Pacific subtropical gyre (NPSG) is characterized by low concentrations of biolimiting nutrients (particularly nitrate and phosphate), low biomass, and generally low rates of new and export production. The upper water column is strongly stratified to the extent that the mixed layer is vertically separated from reservoirs of nutrients that accumulate at depth as a result of microbial degradation of sinking organic matter (Karl and Letelier 2008). In most cases in the oligotrophic gyres, if waters from below the nutricline are introduced to the well-lit surface ocean, a phytoplankton bloom will develop (Dore et al. 2008; McAndrew et al. 2007; Wilson and Qiu 2008). This biological response serves as the basis for the use of wave-driven upwelling as a means to enhance primary productivity and the export of organic carbon to depths exceeding that of the thermocline. The potential that ocean productivity and carbon sequestration can be manipulated is the motivation for the use of these pumps as a geoengineering tool (Kirke 2003; Lovelock and Rapley 2007). However, recent open ocean in situ perturbation experiments have demonstrated a number of unintended ecological responses (Watson et al. 2008). Furthermore, if carbon export is indeed stimulated, it can be difficult to verify its magnitude in a dynamic fluid environment (Powell 2008; Zeebe and Archer 2005). Karl and Letelier (2008) have outlined a careful consideration of the potential response of the surface ocean to controlled artificial upwelling; they have also recommended an appropriate testing site, source water depths, and details of an experiment to verify whether artificial upwelling generated by these pumps could measurably stimulate productivity. Such consideration of the chemical composition of the source water and knowledge of the resident phytoplankton community is critical to ensure that deep water nutrient additions are sufficient to stimulate productivity in excess of the C inputs (Yool et al. 2009). Following this outline, we conducted OPPEX in the early summer of 2008, in the oligotrophic waters of the NPSG.

OPPEX was designed both as an engineering test of the feasibility of wave-driven upwelling and as a field experiment to test the hypothesis of Karl and Letelier (2008). This hypothesis states that artificial upwelling can stimulate organic carbon export in excess of inorganic

carbon inputs via the sustained delivery of water from depth horizons containing excess phosphorus (P) relative to the Redfield ratio of 106:16N:1P. It was put forth as a potential mechanism to explain the enigmatic N_2 fixation–supported blooms (Dore et al. 2008; Karl et al. 1997; White et al. 2007; Wilson and Qiu 2008) that are periodically observed in summer months near the time series station A Long-term Oligotrophic Habitat Assessment (ALOHA), 22°45'N, 158°00'W. These blooms are typically composed of the colony-forming N_2 fixer *Trichodesmium* or symbioses of the heterocystous N_2 fixer *Richelia* and its diatom hosts (Dore et al. 2008). The underlying principles of this hypothesis are that the upwelling of deep water with $N:P < 16$ will lead to 1) rapid photosynthetic assimilation of inorganic N and P in a ratio of approximately 16N:1P, ending with N depletion and residual, unutilized P, and 2) this residual P will stimulate N_2 -based (i.e., diazotrophic) growth given a well-stratified water column (Fig. 2). For the proposed experimental site, in the NPSG, and the horizon of the source water for upwelling (300 m), both bloom stages are theoretically required to achieve net carbon sequestration. Guided by this hypothesis, OPPEX had three primary objectives: 1) to verify the structural integrity and assess the performance of commercially available wave pumps, 2) to develop a monitoring and sampling strategy appropriate for tracking the pumps and the upwelled water for the duration of a deployment in waters north of the Hawaiian islands, and 3) to study the biological response of the system. A combination of autonomous gliders, satellite imagery, and ship-based sampling was used to achieve the latter two objectives. This project was filmed by Impossible Pictures (United Kingdom) for an episode (“Hungry Oceans”) of the Discovery Channel series *Project Earth* (available online at <http://www.discovery.com>). Their programs, such as “Hungry Oceans”/*Project Earth*, reach more than 1.5 billion subscribers in 170 countries.

2. Methods

a. Pump assembly

The components for each of three 300-m-long wave pumps were obtained from Atmocean Inc. Each pump kit consisted of a cylindrical ionomer foam surface float (1-m diameter, 1.83-m length) with an eye bolt on each end; two 0.75-m diameter \times 150-m length sections of polyethylene “tubing” surrounding a 150-m length of $\frac{3}{8}$ -in. vinyl-coated cable; a coupler to connect the two lengths; a set of five nylon ratchet straps; and associated hardware, including keel to affix the tube assembly to the surface float and the valve at the base (Fig. 1). The

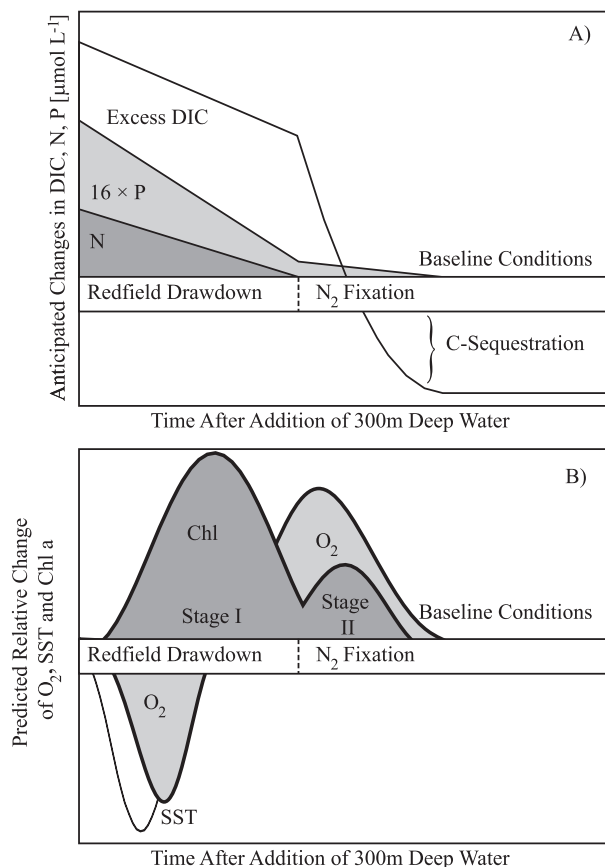


FIG. 2. Illustration of the anticipated biochemical response of wave-driven upwelling of nutrient-rich water from 300 m. Deep water injections will (a) add N, P, and DIC to surface waters and (b) result in a brief and small sea surface temperature (SST) diversion and the introduction of poorly oxygenated water. Phytoplankton chlorophyll (chl) is expected (b) to increase exponentially (a) as organisms draw down these nutrients in a ratio of 106C:16N:1P (i.e., the Redfield ratio, stage I). Given the ratio of N:P derived from 300 m, (a) N will be exhausted first, leaving residual P that will fuel a stage II bloom of N_2 fixing organisms that are predicted to remove the remaining excess DIC and lead to net CO_2 sequestration. (b) The result of these combined blooms will be a slow increase in O_2 derived from net primary productivity.

valve, coupler, and keel were constructed of stainless steel by Atmocean. The vinyl-coated cable connected the surface float to the valve at the base of the tube. Each pump was assembled at the University of Hawaii by connecting two 150-m sections of tubing via a coupler. Each of these 300-m lengths was then wound into a roll with the coupler in the center for ease of deployment. Both a single- and a dual-pump configuration were assembled, whereas the dual-pump array consisted of two single pumps held together by a 100-m section of 1.5-in.-diameter polypropylene line. This tether attached to one end of each buoy. Notably, the single pump and one of the dual pumps were outfitted with a coupler at the

surface, whereas the second dual pump was secured to a float ring.

Several modifications were made to the pumps to improve the chances of a successful experiment. Light, radio, and satellite beacons were installed on each pump system in custom-fabricated capsules that were tightly secured in holes bored into the foam surface buoys. The keel provided by the manufacturer was reinforced to maintain buoy stability. To this end, a more traditional keel was fabricated using $\frac{1}{2}$ in. chain that was strung from one eye of the buoy to the other, directly underneath the line of beacons on top of the buoy. The chain was fastened to these eyes using shackles and turnbuckles, so they could be tightened hard against the buoy, indenting it on the corners and preventing it from rotating. Last, swivel shackles were installed at each of the connection points along the cable interior to the pump. This was done to ensure that any twisting tendencies created by currents, recovery lines, or even the operation of the pump itself could be controlled by allowing the pump to rotate around the vertical axis of the cable.

Each pump was outfitted with two temperature sensors at the top coupler or float ring (15 m), at the midpoint coupler (165 m), and one at the bottom valve (315 m). Last, a NOBSKA three-axis modular acoustic velocity sensor (MAVS 3) was connected to the cable of the single pump just below the top coupler. This instrument was included in the sensor suite as a means to record net upward flow.

b. Deployment

The single and dual pumps were deployed within 2 nautical miles (n mi) of each other on 31 May 2008 at 22.2°N, 157.38°W from the R/V *Kilo Moana*. This location was selected, because prevailing currents ($<0.25 \text{ m s}^{-1}$) in the region are relatively modest (Firing et al. 1999), ensuring that the pumps would not travel outside of the range of available ship time. Also, altimetry data at the time of deployment did not indicate the presence of persistent cyclonic (anticlockwise) eddies that might confound our interpretation of potential upwelling (data not shown). Finally, wave energy in the region is generally considered to be sufficient and favorable for artificial upwelling (Liu and Jin 1995). The mean annual significant wave height for the region is ~ 2.4 m (National Data Buoy Center station 51001).

There were four main components to each pump system: the surface buoy, the tube system with cable inside and couplers attached at midpoint and top, the valve at the bottom, and the recovery line with floats. At sea, all components were fully connected prior to deployment. The buoy was rigged with tie points and release links on both ends and attached to the pump via

the 15-m extension cable. The bottom valve was secured to the pump tubing. A 366-m recovery line was then wound onto the ship's winch and attached to the bottom valve. With the system connected and all sensors in place, the ship's speed was held at 2 kt for the deployment. The buoy was lifted and released into the water first, followed by the careful lowering of the top coupler containing the temperature and current sensors. Once the top part of the tube and buoy were streaming behind the ship, the wound mass of the tube was pushed off the deck. Each pump tube had been assembled such that the upper and lower sections of tubing were wound around the middle coupler. This was done so that the tubes would unwind in the water by the forward motion of the ship and the drag of the material in the water (Fig. 3). The valve end of the pump and the recovery line were held at the edge of the deck until the tube fully unrolled. Once the tube had fully unwound, the valve was lowered into the water, a string of floats was attached to the terminal end of the recovery line, and the entire system was released. The first of the dual pumps was deployed valve first, and the buoy and tether were released after the tube unwound. Only the second of the dual pumps had a recovery line. The elapsed time between release of the buoy and the recovery line was 16 min for the single pump and 35 min for the dual pump (additional details and images of the pump deployment available online at <http://hahana.soest.hawaii.edu/oppex/>).

c. Sampling strategy

To monitor the effect of the pumps on the surrounding environment in the time between deployment and recovery (31 May–14 June 2007), three autonomous Seagliders (iRobot, Bedford, Massachusetts) were launched to map the environmental properties of the water around the drifting single and dual pumps. It was assumed that the drag of a 300-m pump would ensure that prevailing surface currents in the region would move faster than the pumps and any upwelled water would spill over the top coupler to its equilibrium depth and then be carried downstream. For this reason, the mission of the Seagliders was primarily to survey the downstream path of the pumps in a directed pattern. Vertical profiles were obtained as each glider alternately descended and ascended to a depth of 500 m in a sawtooth pattern. Individual dives (surface to 500 m and back) covered ~ 1.6 km of horizontal distance and were approximately 3 h in duration. Each Seaglider was equipped to measure particle scattering, chlorophyll fluorescence, dissolved oxygen, pressure, temperature, and salinity. The anticipated sign of many of these properties in response to upwelling is noted in Fig. 2. For dissolved oxygen data,

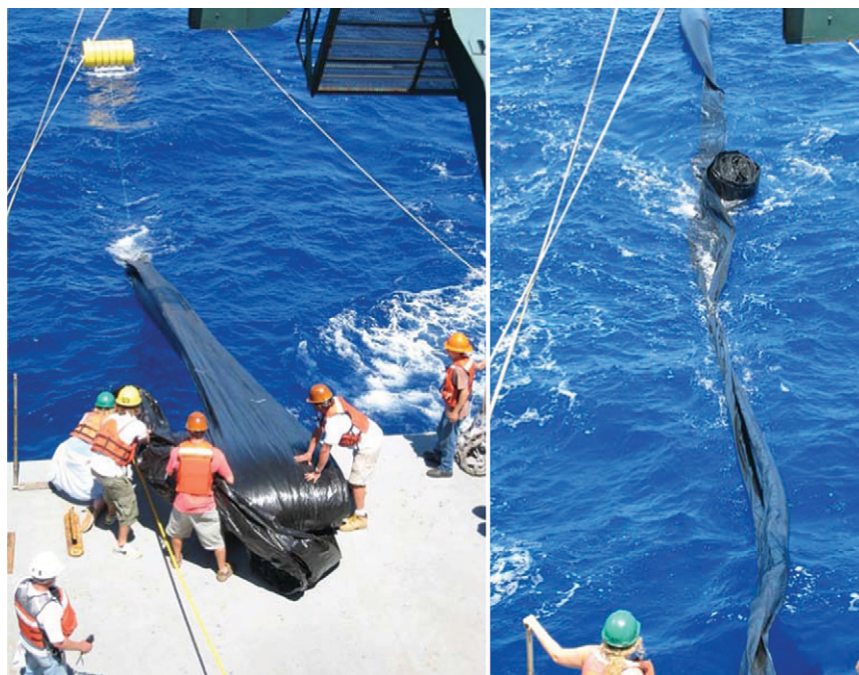


FIG. 3. Image of the deployment of the single pump. With the ship moving forward at 2 kt, the buoy of the single pump was deployed. The main masses of the pumps were then deployed with the bottom valve of the pump system secured on deck. The forward motion of the ship causes the tube to slowly unwind to achieve full length. After it was fully opened, the valve and recovery line were deployed.

only the downcast data were used for analysis of blooms as increased variability was observed on upcasts. Gliders were also fitted with an acoustic transponder and GPS/Iridium antenna/system (location and communications). Geolocational and biochemical data were transmitted to the University of Hawaii base station between dives while the glider was at the ocean surface. Remotely sensed, real-time Moderate Resolution Imaging Spectroradiometer (MODIS) chlorophyll-*a* and sea surface temperature (1-km resolution) as well as sea surface height anomalies and wave forecast data were monitored over the course of this experiment.

Direct measurements of the biogeochemistry of the waters surrounding the pumps were conducted within 12 h prior to pump deployment and before the pumps were recovered. Profiles of temperature, salinity, dissolved oxygen, and *in vivo* chlorophyll were obtained via deployment of a rosette package mounted with a Sea-Bird conductivity-temperature-depth (CTD), a fluorometer, and an oxygen sensor. Discrete samples were collected from multiple depths for analysis of extracted chlorophyll-*a*, dissolved inorganic carbon, and dissolved oxygen concentrations and nutrients (all protocols at <http://hahana.soest.hawaii.edu/hot/protocols>). Finally, a towed video plankton recorder (VPR; WHOI) was used to map the

upper water column around the pumps during the recovery cruise in search of low temperature, low oxygen, or high chlorophyll features (Fig. 2b) that may have originated from the pumps.

3. Results

a. Postdeployment monitoring phase

Ship time, scheduling, and funding restrictions prohibited direct ship-based monitoring of the pumps for the duration of the deployment. For this reason, gliders and remote sensing data were used to track ocean properties for the two-week period between deployment and the scheduled recovery of the pumps. Initially, the gliders were directed northwest of the pumps to ensure that they were not damaged by ship operations. Following the successful deployment of the pumps, each of the three gliders was mobilized to transverse the upstream and downstream paths of the pumps. It required approximately 4 days for the gliders to transit to the pumps (Fig. 4). In these first few days, one of the three gliders experienced pitch control anomalies that precluded its use as a profiling instrument. For this reason, it was kept at the surface and was subsequently used as

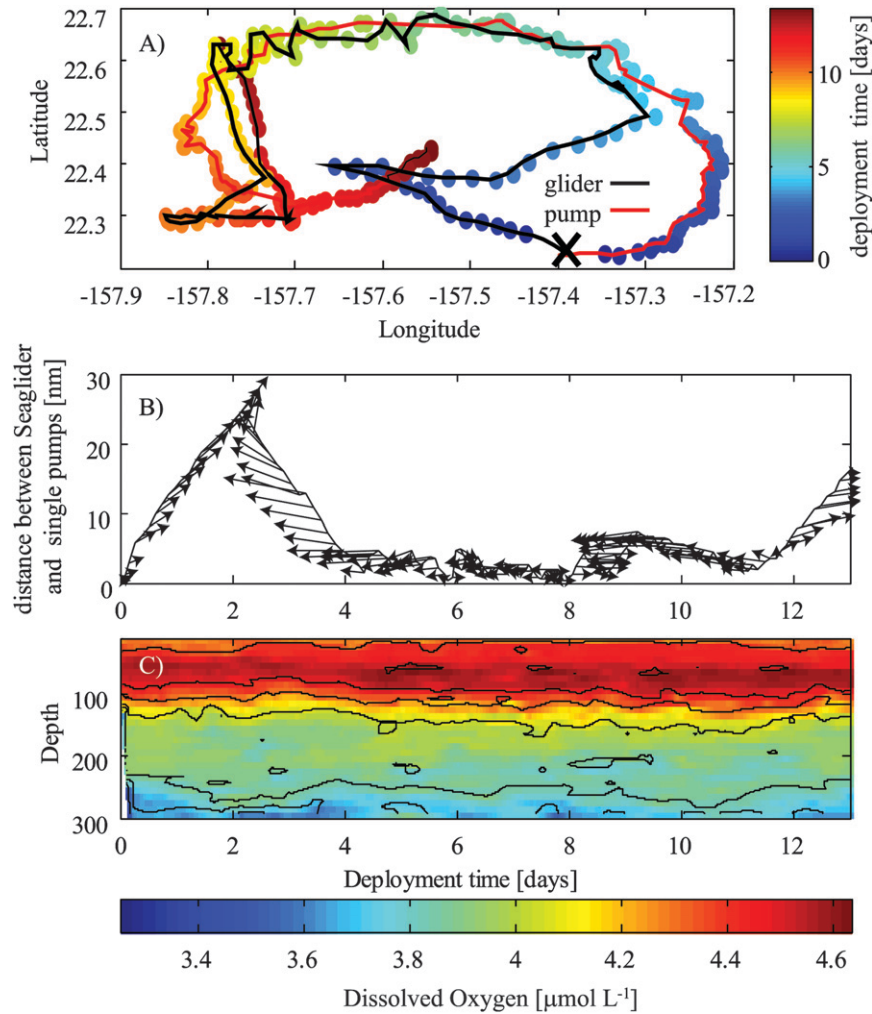


FIG. 4. (a) Surface map of the trajectory of the single pump (red line) and the primary Seaglider (thick line). The deployment site is marked by a cross. Contours correspond to the deployment time in days. (b) The distance of the primary Seaglider from the single pump over the course of the experiment. Arrows indicate the bearing toward the pump from the Seaglider. (c) Contours of dissolved oxygen concentrations measured on the downcast of each Seaglider dive.

a surface drifter to estimate the trajectory and speed of local surface currents. Real-time data derived from glider-mounted sensors did not indicate any significant change in surface properties such as dissolved oxygen (Fig. 4c), temperature, chlorophyll, or scattering (data not shown) that could be attributed to artificial upwelling as per the trajectory of changes expected (Fig. 2). At the time, we could not be certain if the null result was due to the fact that we were not sampling the appropriate phase of the potential bloom or sampling near enough to the pumps or if the pumps were not operational. Remote sensing of surface chlorophyll (available online at <http://picasso.oce.orst.edu/ORSOO/hawaii/pumps/>) also did not reveal any persistent features that

could be identified as originating from localized artificial upwelling.

b. Pump recovery

The second cruise aboard the R/V *Kilo Moana* embarked to revisit the pumps on 12 June 2008. On 13 June, divers entered the water and recovered the temperature sensors located in the top coupler of each of the pumps (single and dual). During these underwater operations, divers observed that the top sections of tubing material of both the single and dual pumps were extensively torn. At this point, it was not clear to what extent the pumps had been damaged. To assess whether deep water was still being delivered to the midcoupler (165 m) or if

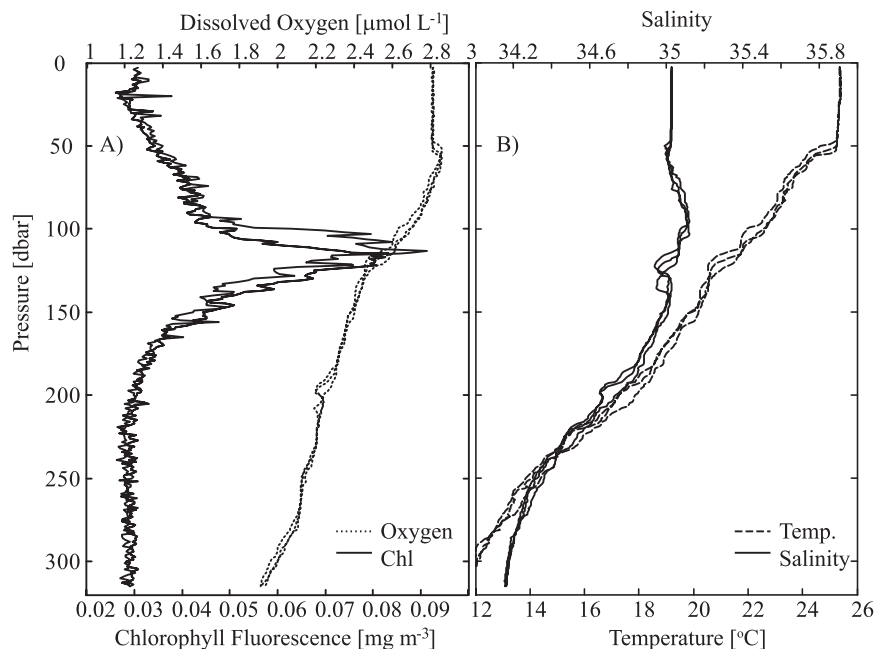


FIG. 5. (a) Dissolved oxygen, chlorophyll fluorescence and (b) temperature and salinity derived from multiple CTD casts around the single pump just prior to recovery.

a biochemical signal of deep water delivery was evident (Fig. 2), a series of 3–4 CTD casts were performed around the single and dual pumps. Casts were conducted as close to the pumps as deemed safe by the ship's captain (~ 1 n mi). Temperature, salinity, dissolved oxygen, and chlorophyll-*a* profiles were not only relatively invariant in the regions surrounding the pumps (Fig. 5) but were not significantly changed from predeployment conditions. The VPR was deployed to map the chlorophyll field in the upper mixed layer (20–60 m) downstream (< 20 n mi) of the single pump. The resultant data show chlorophyll distributions closely following isothermal surfaces. Surface blooms were not observed along this transect (data not shown).

Following completion of all CTD surveys and the VPR deployment, the entire length of the single pump was recovered and all remaining sensors (thermistors, MAV3 current meter) were retrieved. During this recovery process, catastrophic failure of materials was evident. Several of the straps that were used to hold the shackles to the buoy were severed, apparently by frictional forces. The metal keel designed by Atmocean was partially separated. The tube material was extensively torn and chafed and was completely separated from the top of the midpoint coupler. The midpoint coupler itself had disconnected from the central cable as the internal support rods of the couplers were shorn away from the cylinder walls. Along with the tube material that was connected to the bottom section, the midpoint coupler

wall had fallen to the depth of the valve. The amount of time spent recovering this mass of torn tubing and twisted metal ultimately prohibited the immediate recovery of the similarly damaged dual-pump array. This task was diverted to a later cruise scheduled in the area. Nonetheless, the sensors from the top coupler of the dual pump were recovered by the dive team.

c. Temperature records

Inspection of the temperature records obtained from the single pump revealed that, despite the eventual materials failure, the pump had successfully delivered cold water from 315 m to the top coupler for a period of ~ 17 h (Fig. 6). Using the thermistor data and the CTD temperature profiles, we were able to reconstruct the timeline of events for this pump. Taking the CTD temperature data as a depth proxy ($11^{\circ}\text{C} = 315$ m, $18.7^{\circ}\text{C} = 165$ m, and $25.3^{\circ}\text{C} = 15$ m), we found that the valve sank to 315 m within 30 min of deployment. Within an hour after the pump had reached its target depth, both midcoupler-mounted thermistors recorded temperatures 2°C below expected for water at 165 m. In another two hours time, temperatures at the top coupler were depressed by greater than 1°C relative to the surrounding water (Fig. 6). Given the temperature of the source water at 315 m (11°C , Fig. 6), it is apparent that significant conductive heat exchange across the pump walls occurred during the upwelling process. The magnitude of this loss (13°C) is in agreement with calculations

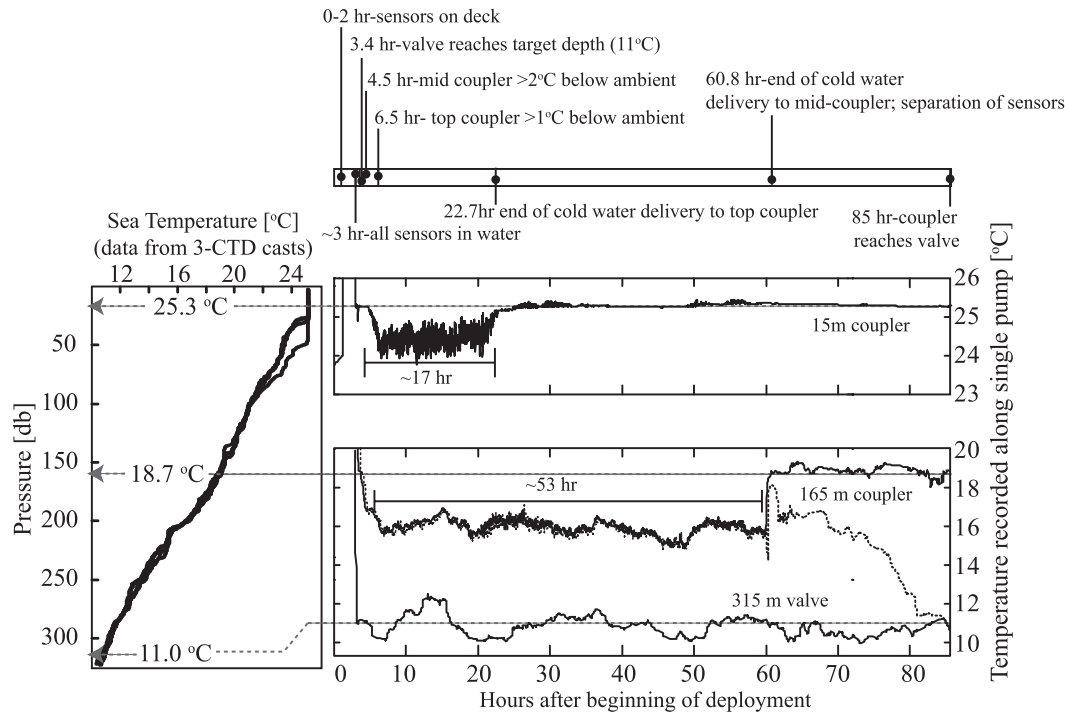


FIG. 6. (left) Profile of water column temperature from three concurrent casts using a rosette-mounted SeaBird CTD collected just prior to the deployment of the single pump. (top right) Timeline of events for the single pump. Values denote the hour that each event was recorded. (middle right) Time series of temperature recorded the top coupler, 15 m; (bottom right) the midcoupler, 165 m; and the bottom valve, 315 m.

assuming the thermal conductivity (k) of polyethylene to be $0.33 \text{ W m}^{-1} \text{ K}^{-1}$ (thickness = 0.0032 m ; Leinhard and Leinhard 2000). Specifically, if we iteratively calculate the temperature change (ΔT) for each meter of depth from Fournier's law and the equation for specific heat using the temperature record from CTD profiles, we predict a 11.4°C warming over a 300-m transit [$\Delta T = Q t m c^{-1}$, where $Q = (\text{pump area} \times k \times \text{material thickness}^{-1}) \times (T_{\text{outside}} - T_{\text{inside}})$; specific heat (c) = $3850 \text{ J (kg } ^\circ\text{C}^{-1})$, and the mass of water (m) is calculated for 1-m intervals with a time step (t) equivalent to the measured transit time of 0.028 m s^{-1}]. This corresponds to a temperature at 15 m of 24.5°C , which is quite similar to actual temperature records at 15 m ($\sim 24^\circ\text{C}$). This effect, the diffusion of temperature (but not salinity) is described mathematically by Stommel et al. (1956) as the "perpetual salt fountain."

After this initial 17-h period of artificial upwelling, temperatures at the top coupler returned to values typical of 15 m, thus indicating materials failure in the portion of the tube above the midpoint coupler. Cold water delivery to the 165-m coupler continued for $\sim 53 \text{ h}$, after which time the sensor records at this depth diverge, with the one temperature sensor recording the freefall of the coupler to the depth of the valve and the other sensor recording

the cessation of upwelling (Fig. 6). These records are consistent with the attachment point of each sensor, with one being secured to the cable at 165 m and the other on the support rod of the coupler.

Only the thermistors from the top coupler of the dual pumps were recovered. These data indicate that short-term pulses of cold water reached the surface of the pump with a float ring, whereas the pump attached to a coupler did not function (data not shown). The cold water pulses showed no periodicity nor did they last longer than 2 h. Without the full complement of sensors from this array, we can only speculate as to the cause and timing of the complete failure of these pumps. When available ship time permitted the attempted recovery of the dual pumps, all that remained were the buoys, electronics, keel, chain, and a few of the straps.

d. Estimated upwelling velocity

Using the volume of the single pump (136 m^3) and the elapsed time required for cold water to reach the top coupler ($\sim 3 \text{ h}$, Fig. 6), we estimate the rate of artificial upwelling over the operational phase of deployment to be approximately $45 \text{ m}^3 \text{ h}^{-1}$. Independent of the assumptions made above, the MAV3 current meter provides a measure of vertical velocities recorded at the

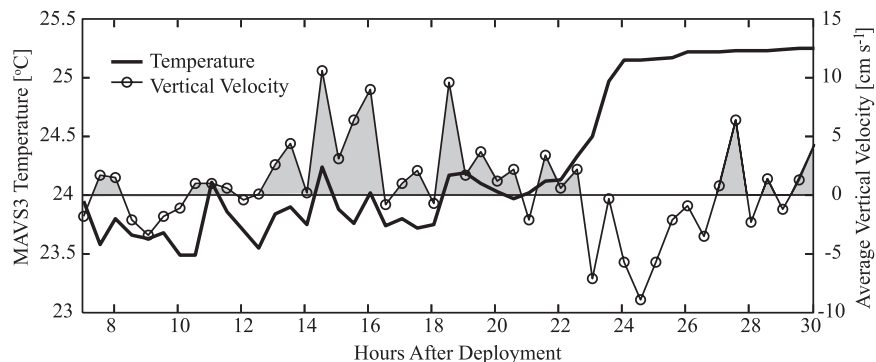


FIG. 7. Time series of vertical velocity recorded by the MAV3 sensor in the top coupler of the single pump relative to this sensor's temperature record. Shaded regions represent phases of net upwelling (positive vertical velocity). The mean flow for the period prior to cessation of cold water delivery was $+2 \text{ cm s}^{-1}$.

center of the pump. Although this meter was badly damaged at some time during the 2-week deployment, the data were salvageable. The MAV3 was installed just below the top coupler of the single pump. The orientation of this meter was such that upward (downward) flow was recorded as positive (negative). The meter was programmed to sample for 8.5-min bursts separated by 21.5-min gaps, a scheme chosen to avoid biasing by the wave period ($\sim 6 \text{ s}$, wave height = 1.5 m from nearest National Data Buoy Center station, 51001). Given that the water passing over this sensor is ultimately constrained by the walls of the tube, we can disregard horizontal flow (across the same plane as the sensor heads) and angular deviations from the vertical plane.

For each sampling burst, vertical velocities were normally distributed with a range of negative to positive values. Data from each burst period were filtered to remove anomalous records greater than three standard deviations (three passes). The mean vertical velocity was then calculated for each sampling burst. For the period that cold water was recorded at the top coupler ($\sim 6\text{--}23 \text{ h}$ after deployment), the mean vertical velocity was 2 cm s^{-1} (1728 m day^{-1} ; Fig. 7). This vertical velocity is orders of magnitude greater than estimates of the natural upward vertical velocity for the Pacific Ocean basin, 0.012 m day^{-1} (Munk 1966). Using the area of the coupler (0.45 m^2) and this net upward velocity of 2 cm s^{-1} , the MAV3 data indicate a volumetric upwelling rate of approximately $32 \text{ m}^3 \text{ h}^{-1}$. However, if we consider that the Reynolds number derived from this flow rate is ~ 100 , the flow regime may have been laminar. In this case, the velocity distribution across the tube would be parabolic and the velocity measured by the MAV3 at the center of the tube would be twice the mean velocity for the entire cross section. Thus, we can assign a lower limit of $16 \text{ m}^3 \text{ h}^{-1}$ to the observed rate of upwelling. The range of upwelling rates derived from these independent

measures (temperature-based and net upward velocity) is then $16\text{--}45 \text{ m}^3 \text{ h}^{-1}$.

e. Estimated nutrient delivery

Over the course of this experiment, deep water upwelling persisted for a period of 17 h at a rate of $\sim 45 \text{ m}^3 \text{ h}^{-1}$. Given the known nutrient concentrations of these source waters relative to the values observed in the mixed layer [as given by Karl and Letelier (2008): $76 \mu\text{mol L}^{-1}$ dissolved inorganic carbon (DIC), $9.93 \mu\text{mol L}^{-1}$ nitrate (NO_3), and $0.695 \mu\text{mol L}^{-1}$ phosphate (PO_4)] and the maximum estimated volume of water upwelled ($17 \text{ h} \times 45 \text{ m}^3 \text{ h}^{-1} = 765 \text{ m}^3$), we can estimate the potential nutrient enrichments that may have occurred during this trial. If we consider a modest enrichment area of 100 m^2 and the depth of the surface mixed layer (45 m), the total NO_3 and PO_4 enrichment in the absence of biological drawdown would have been on the order of 17 and 1 nmol L^{-1} , respectively. Although these projected NO_3 values are greater than the mean summer surface values observed in the region ($\sim 3 \text{ nmol L}^{-1}$), projected PO_4 values are at detection limits (1 nmol L^{-1}). If we convert the full aliquot of potentially upwelled DIC ($0.13 \mu\text{M}$) to phytoplankton biomass using a mean C:chlorophyll ratio of 50 g:g (MacIntyre et al. 2002), we would expect an increase in chl on the order of $0.0002 \mu\text{g L}^{-1}$, a value that is within the standard error of fluorometric chlorophyll analyses for the region (typical standard deviation for surface chlorophyll at station ALOHA = $0.008 \mu\text{g L}^{-1}$). Mean nutrient concentrations and analytical precision are derived from Hawaii Ocean time series data.

4. Conclusions

Two main outcomes arise from this field experiment: 1) significant reengineering of existing wave pump

technology is necessary for open ocean applications and 2) the difficulties inherent in tracking a biochemically evolving mass of water are significant and cannot be underestimated. In addition to these issues, the scale and duration of a biological response will certainly vary with season, region, and a myriad of other factors. In that regard, we believe that any proposed strategy to intentionally perturb marine ecosystems using artificial upwelling is premature and should be avoided until the sign and magnitude of potential outcome scenarios can be verified for a given habitat (Buesseler et al. 2008).

The most salient and repairable outcome of OPPEX was materials failure. By all measures, the tube material, the welds, and the keel were structurally insufficient to survive the forces encountered in an open ocean deployment. Despite our efforts to strengthen the commercial product prior to deployment, we were only able to document short-term (≤ 17 h) delivery of deep water for two of the three pumps prior to cessation of upwelling. A cascade of materials failure occurred after this time, culminating in the loss of the dual pumps. The endurance of future wave pumps will need to be enhanced, a more durable tube material is required and the keel design will need to be reengineered before future experiments are conducted.

Although the point source vertical velocities generated by these pumps (~ 1728 m day $^{-1}$) are orders of magnitude greater than natural upwelling rates (0.012 m day $^{-1}$), we were not able to determine the settling depth or the horizontal distribution of the water that was upwelled by the combination of the wave pumps. This information will be vital to a determination of the probability of a biological response such that the sufficient deep water enrichments must be entrained within the euphotic zone to ensure sufficient light for bloom development (Fennel 2008; Letelier et al. 2008). All available calculations (I. Ginis 2008, personal communication) suggest that this will be the case; nonetheless, the settling depth and horizontal penetration of deep water will need to be verified in future field experiments. The data from the gliders, towed VPR, and remote sensing did not detect features that were clearly distinguishable from the natural variability of the region (e.g., Figs. 4c, 5). This uncertainty is not entirely unexpected, given the scale of operation (1–2 pumps operating for < 3 days); however, it highlights the difficulties that are faced when trying to identify a biological response in a heterogeneous and fluid environment.

Additionally, it is not clear that wave pumps can perform as efficiently as predicted by mathematical models (Liu and Jin 1995; Vershinsky et al. 1987). For the period that successful upwelling was achieved, the measured upwelling velocities (0.013 m 3 s $^{-1}$) are an

order of magnitude less than what Liu and Jin (1995) have predicted (0.45 m 3 s $^{-1}$) for wave pumps with similar dimensions ($d = 1.2$ m, length = 300 m) and experiencing similar wave heights (1.9 m). Moreover, given that the mean wave height for the deployments was 1.5 m and the dominant wave period was 6 s, a vertical velocity of 25 cm s $^{-1}$ would represent perfectly efficient utilization of regional wave energy. The observed upwelling velocity (2–3 cm s $^{-1}$) indicates that the pumps operated at $\sim 10\%$ efficiency. Regardless of whether this discrepancy is due to irregularity of wave heights experienced during deployment, rapid failure of materials, or some other undetermined factor, the role that the variability of the physical environment plays (wave height and frequency, storms, etc.) in impacting the performance and survivability of the pumps must be carefully considered prior to long-term tests.

Given the uncertainties of the physical and mechanical factors for wave pump deployments, an alternate approach to studying the *in vivo* biological response of the surface ocean to deep water fertilization could utilize a more proven technology, such as ocean thermal energy conversion (OTEC; Avery and Wu 1994). This approach would not only allow upwelling volumes to be closely regulated, but it would leverage the more extensive research and development that has gone into OTEC technology (Avery and Wu 1994; Takahashi and Trenka 1996) as compared to the relatively nascent efforts to design and maximize the efficiency of wave pumps. A more direct, albeit energy-inefficient approach, would be to use an energy-powered pump to fertilize a patch of water seeded with a transient tracer such as trifluoromethyl sulphur pentafluoride. Although this latter proposal may also face technological challenges, the benefits would be that the source depth could be easily varied and the perturbed water mass more readily identified and monitored over time.

More than an engineering challenge, OPPEX was a test of our ability to identify and track perturbations in a heterogeneous and turbulent ocean. A significant challenge encountered during OPPEX was to predict the path of the pumps and successfully maneuver the gliders to target the potential plume downstream of the pumps. This challenge was heightened by temporal offsets in the relay of geolocational data being transmitted from the pumps and the gliders as well as the spatial uncertainty associated with Argos data ($\pm 1/4$ n mi). At worst, there was an 11-h gap in the time that the most recent Seaglider position was known and when the pump location was relayed. This confounded the effort to efficiently utilize the gliders to track the anticipated path of the pumps. Future experiments of this sort would ideally enable a more complex and adaptive network of

remotely operated and autonomous platforms capable of achieving synoptic domain coverage (Dickey et al. 2008). In this regard, a significant effort is underway to develop “smart” glider technology, enabling fleets of gliders to recognize or identify biochemical features as they are sampled (Abbott and Sears 2006; Dickey et al. 2008). Additionally, programming of environmental or geolocational feedbacks control laws has been proposed to allow gliders to locate and track biochemical features while maintaining coordinated vehicle trajectories and sampling patterns (Bhatta et al. 2005). This effort is a prime example of an opportunity for the cooperation of oceanographers, engineers, and programmers to revolutionize our knowledge of ocean dynamics.

In sum, despite the failure of this experiment to generate a measurable biological response, we have shown that the underlying principal of this technology is sound. Wave pumps can transport deep, nutrient-rich water to the surface ocean. From this valuable experience, we can formulate a few recommendations for the next essential round of trials that may evaluate the capacity for this technology to enhance oceanic carbon sequestration. Key improvements will need to foremost consider the cost and methods needed to monitor the pumps from the time of deployment to the time that carbon sequestration could potentially be measured. In our experiment, we faced challenges with the temporal offset of the Argos tracking system on the pumps and the difficulty of redirecting the gliders to intercept the anticipated location of potentially perturbed water masses. This issue could partially be resolved by an investment in commercially available products with near-real-time communications capability (e.g., Iridium, Global Star, or Orbcomm). However, this will not address the inherent unpredictability of the physical dynamics of wave-driven upwelling. The horizontal trajectory as well as the settling depth of the upwelled water will need to be tracked. As has been suggested for the next round of iron fertilization trials, we would recommend that the second generation of wave pump experiments adopt a more comprehensive monitoring scheme than we were able to conduct. This should involve a combination of gliders, remotely operated vehicles, deployment of surface and subsurface drifters, and a more prolonged ship presence. It may also be necessary to reconsider the size or spacing of pumps. If technologically feasible, a much larger diameter pump or some configuration of multiple pumps would enhance the total volume of water and nutrients upwelled and may generate a larger bloom. This will be key as the probability of bloom detection increases with the scale of the perturbed patch. For iron fertilization trials, target patch sizes are on the order of hundreds of square kilometers (Watson et al. 2008).

Substantial changes in pump configurations will be needed to meet such targets. If followed, these recommendations would significantly increase costs and require additional investments of personnel, tracking, and monitoring technology and the scale of logistics coordination needed.

Our experiment was intended to be a small-scale test of a recent hypothesis regarding the successional response of pelagic ecosystems. The sampling and engineering challenges encountered illuminate the uncertainties that will inevitably be faced when trying to manipulate the natural environment. The ultimate response of the ecosystem is anticipated to vary with location, season, source water composition, and the rate and phasing of upwelling. Moreover, the initial conditions of the microbial community prior to upwelling, the composition and concentration of macronutrients and micronutrients that are delivered via upwelling, and the prevailing physical regime will interact to define the outcome of such experiments. We believe that these pumps can be used as a tool to test our understanding of the marine environment. However, the inherent complexity of the pelagic habitat and the variability of the ecosystem response to artificial upwelling cannot be dismissed. In a changing climate, it is more imperative than ever to study nature by developing well thought out in situ experiments. The results of this audacious field experiment serve as a reminder of the difficulties we face in this endeavor.

Acknowledgments. We thank the National Science Foundation (C-MORE; Award EF-0424599) and the Gordon and Betty Moore Foundation for their generous funding. Additionally, we are grateful to the Discovery Channel and Impossible Pictures for donating several of the pumps for this experiment, contributing funds to secure the necessary ship time, and documenting our efforts and sharing our science with the general public. This research could not have been conducted without the support and expertise of the captain and crew of the R/V *Kilo Moana* and UH Diving safety personnel. We also thank Cabell Davis and Josh Eaton for their invaluable work with the VPR, and Phil Kithil and Brian von Herzen for their contributions to the overall evolution of this project. Yvette Spitz and two anonymous reviewers provided valuable comments to improve this manuscript.

REFERENCES

- Abbott, M., and C. Sears, 2006: The always connected world and its impacts on ocean research. *Oceanography*, **19**, 14–21.
- Avery, W. H., and C. Wu, 1994: *Renewable Energy from the Ocean: A Guide to OTEC*. The Johns Hopkins University/Applied

- Physics Laboratory Series in Science and Engineering, Oxford University Press, 480 pp.
- Bhatta, P., and Coauthors, 2005: Coordination of an underwater glider fleet for adaptive sampling. *Proc. Int. Workshop on Underwater Robotics*, Genoa, Italy, International Advanced Robotics Programme, 61–69.
- Buesseler, K. O., and Coauthors, 2008: Ocean iron fertilization—Moving forward in a sea of uncertainty. *Science*, **319**, 162.
- Dickey, T. D., E. C. Itsweire, M. A. Moline, and M. J. Perry, 2008: Introduction to the Limnology and Oceanography special issue on autonomous and Lagrangian platforms and sensors (ALPS). *Limnol. Oceanogr.*, **53**, 2057–2061.
- Dore, J., R. Letelier, M. Church, R. Lukas, and D. Karl, 2008: Summer phytoplankton blooms in the oligotrophic North Pacific Subtropical Gyre: Historical perspective and recent observations. *Prog. Oceanogr.*, **76**, 2–38.
- Fennel, K., 2008: Widespread implementation of controlled upwelling in the North Pacific Subtropical Gyre would counteract diazotrophic N₂ fixation. *Mar. Ecol. Prog. Ser.*, **371**, 301–303.
- Firing, E., B. Qiu, and W. Miao, 1999: Time-dependent island rule and its application to the time-varying North Hawaiian Ridge Current. *J. Phys. Oceanogr.*, **29**, 2671–2688.
- Isaacs, J. D., D. Castel, and G. L. Wick, 1976: Utilization of the energy in ocean waves. *Ocean Eng.*, **3**, 175–187.
- Karl, D., and R. Letelier, 2008: Nitrogen fixation-enhanced carbon sequestration in low nitrate, low chlorophyll seas. *Mar. Ecol. Prog. Ser.*, **364**, 257–268.
- , and Coauthors, 1997: The role of nitrogen fixation in biogeochemical cycling in the subtropical North Pacific Ocean. *Nature*, **388**, 533–538.
- Kenyon, K., 2007: Upwelling by a wave pump. *J. Oceanogr.*, **63**, 327–331.
- Kirke, B., 2003: Enhancing fish stocks with wave-powered artificial upwelling. *Ocean Coastal Manage.*, **46**, 901–915.
- Leinhard, J. H., and J. H. Leinhard, 2000: *A Heat Transfer Textbook*. Phlogiston Press, 760 pp.
- Letelier, R., P. Strutton, and D. Karl, 2008: Physical and ecological uncertainties in the widespread implementation of controlled upwelling in the North Pacific Subtropical Gyre. *Mar. Ecol. Prog. Ser.*, **371**, 305–308.
- Liu, C., and Q. Jin, 1995: Artificial upwelling in regular and random waves. *Ocean Eng.*, **22**, 337–350.
- Lovelock, J. E., and C. G. Rapley, 2007: Ocean pipes could help the Earth to cure itself. *Nature*, **449**, 403.
- MacIntyre, H. L., T. M. Kana, T. Anning, and R. J. Geider, 2002: Photoacclimation of photosynthesis irradiance response curves and photosynthetic pigments in microalgae and cyanobacteria. *J. Phycol.*, **38**, 17–38.
- McAndrew, P. M., K. M. Björkman, M. J. Church, P. J. Morris, N. Jachowski, P. J. le. B. Williams, and D. M. Karl, 2007: Metabolic response of oligotrophic plankton communities to deep water nutrient enrichment. *Mar. Ecol. Prog. Ser.*, **332**, 63–75.
- Munk, W. H., 1966: Abyssal recipes. *Deep-Sea Res.*, **13**, 207–230.
- Powell, H., 2008: What are the possible side effects? *Oceanus*, **46**, 14–17.
- Stommel, H., A. B. Arons, and D. Blanchard, 1956: An oceanographic curiosity: The perpetual salt fountain. *Deep-Sea Res.*, **3**, 152–153.
- Takahashi, P., and A. Trenka, 1996: *Ocean Thermal Energy Conversion*. John Wiley, 75 pp.
- Vershinsky, N. V., B. P. Psenichnyy, and A. V. Solovyev, 1987: Artificial upwelling using the energy of surface waves. *Oceanology*, **27**, 400–402.
- Watson, A., P. Boyd, S. Turner, T. Jickells, and P. Liss, 2008: Designing the next generation of ocean iron fertilization experiments. *Mar. Ecol. Prog. Ser.*, **364**, 303–309.
- White, A. E., Y. H. Spitz, and R. M. Letelier, 2007: What factors are driving summer phytoplankton blooms in the North Pacific Subtropical Gyre? *J. Geophys. Res.*, **112**, C12006, doi:10.1029/2007JC004129.
- Wilson, C., and X. Qiu, 2008: Global distribution of summer chlorophyll blooms in the oligotrophic gyres. *Prog. Oceanogr.*, **78**, 107–134.
- Yool, A., J. G. Shepard, H. L. Bryden, and A. Oschlies, 2009: Low efficiency of nutrient translocation for enhancing oceanic uptake of carbon dioxide. *J. Geophys. Res.*, **114**, C08009, doi:10.1029/2008JC004792.
- Zeebe, R. E., and D. Archer, 2005: Feasibility of ocean fertilization and its impact on future atmospheric CO₂ levels. *Geophys. Res. Lett.*, **32**, L09703, doi:10.1029/2005GL022449.